

Heteroatoms moving protons: Synthetic and mechanistic studies of bifunctional organometallic catalysis*

Douglas B. Grotjahn

Department of Chemistry and Biochemistry, San Diego State University, 5500 Campanile Drive, San Diego, CA 92182-1030, USA

Abstract: Improved organometallic catalysts resulting from including ligands capable of proton transfer or hydrogen bonding are described. Pyridyl- and imidazolylphosphines accelerate *anti*-Markovnikov alkyne hydration and alkene isomerization and deuteration by factors of 1000 to more than 10000. Evidence for proton transfer and hydrogen bonding in catalytic intermediates comes from computational, mechanistic, and structural studies, where ¹⁵N NMR data are particularly revealing.

Keywords: alkenes; alkynes; bifunctional catalysis; hydrogen bonding; palladium; protons; ruthenium.

INTRODUCTION

The importance of catalysis and catalytic processes cannot be overstated. It has been estimated that 35 % of global gross domestic product depends on catalysis [1]. Catalysis-based chemical syntheses are involved in 60 % of chemical products and 90 % of chemical processes. In the United States, the chemical industry represents 10 % of all manufacturing, and employs more than 1 million people [2]. Solving world needs for clean and renewable energy may hinge on the ability of catalysts to make fuels from sunlight [3]. In short, improving catalysts and uncovering new mechanisms for catalysis could have a large practical impact in many areas.

In any chemical transformation, bonding electrons are moved. Transition metals facilitate bond-breaking and -making using their valence electrons. However, in many catalytic processes, protons are transferred from one atom to another as substrate is transformed to product. Therefore, starting about 10 years ago [4,5] our group began studying combining the ability of a transition metal to move electrons with ligands capable of proton transfer, examples in the wide field of bifunctional catalysis [6]. This article will focus on our studies of phosphines bearing an imidazolyl or pyridyl group and the roles the basic nitrogen substituent can play. Homage is paid to pioneering work at Shell in the 1990s [7,8], where a pyrid-2-yl or 6-methyl-2-pyrid-yl substituent at phosphorus led to very significant enhancements in rate and selectivity for Pd-catalyzed methoxycarbonylation of propyne. A strong acid with weakly coordinating conjugate base (toluenesulfonic acid) was a co-catalyst in this transformation, suggesting that perhaps a pyridinium species was important in the catalytic cycle, though there is more than one possibility for its precise role [9,10]. Despite the attractiveness and novelty of the use of pyridylphosphines noted above, until our work on imidazolyl- and pyridylphosphines there appeared to be no other reports of catalysis using these species. Instead, hundreds of pyridylphosphine complexes

*Paper based on a presentation at the 9th International Conference on Heteroatom Chemistry (ICHAC-9), 30 June–4 July 2009, Oviedo, Spain. Other presentations are published in this issue, pp. 505–677.

[11,12] and fewer imidazolylphosphine complexes (examples, [13–20]) had been made for a variety of purposes other than catalysis. Here, hydrogen bonding or proton transfer in catalysis using heterocyclic phosphines and their complexes will be the focus.

RESULTS AND DISCUSSION

Figure 1 summarizes key relative rate data for catalysis of two reactions, *anti*-Markovnikov alkyne hydration (eq. 1) and alkene isomerization (eqs. 2 and 3), which show the benefits of heterocyclic phosphines. Before our work, complex **1** [21] was the fastest and most selective catalyst for eq. 1. Complexes **2** and **3** are 90 and 1100 times faster, respectively [5,22], and data for aquo analog **4b** show further improvement. For alkene isomerization, an imidazolyl substituent in **6** offers rate accelerations of more than 10000. The significance of *tert*-butylated heterocycles will be described first, before more detailed considerations of hydrogen bonding and proton transfer in the reactions summarized in Fig. 1.

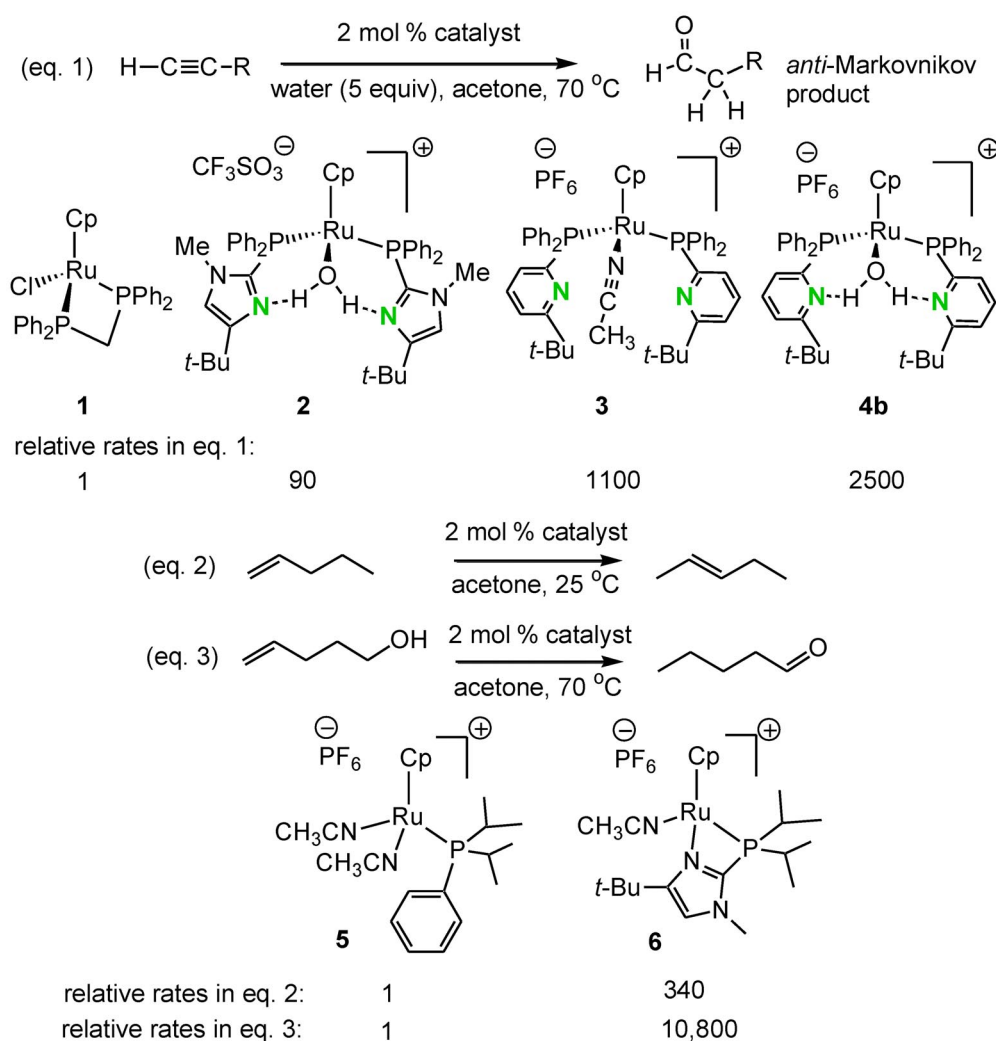


Fig. 1 Comparing bifunctional and standard catalysts in alkyne hydration and alkene isomerization.

Catalyst design considerations

In making potential catalysts with heterocyclic phosphines, there are several design considerations. Figure 2 illustrates the imidazolylphosphine case. A common ground-state catalyst structure would be **7** or **8**. For catalysis, we seek to form **9** for binding with polar ligands (illustrated by water), leading to **10**. Ligand loss from **8** could be adjusted by selecting an appropriately labile co-ligand L, whereas chelate opening in **7** could be adjusted by varying the steric demand of R¹ next to the coordinating nitrogen, as well as by varying the sterics and electronics of the phosphine R groups. In a series of papers in the past 8 years we have provided experimental evidence for the profound role of R¹ in both chelate stability and also catalytic ability [5,22–32], where a *tert*-butyl group often emerges as an excellent choice. For example (Fig. 3), Pd(II) complexes **11a** and **11b** exhibit metal–nitrogen bond lengths of 2.1639(18) and 2.2626(17) Å, for a change of 0.0987(29), respectively, whereas the other three metal–ligand bond distances are unchanged within 0.012 Å [25]. Ruthenium complexes **12a** and **12b** have not been structurally characterized but they show dramatically different reactivity: **12a** is static on the NMR time scale, showing sharp ¹H and ³¹P NMR spectra even at 80 °C, whereas its *tert*-butylated analog exhibits broad NMR resonances even near 0 °C. Moreover, **12a** is ineffective as an alkyne hydration catalyst, whereas **12b** (which becomes **4b** during hydration reactions) shows excellent activity [22,23,33]. Additionally, we note that increasing the size of “innocent” phosphine R groups promotes chelation [25,34], an organometallic manifestation of the Thorpe–Ingold or gem-dialkyl effect [35–38]. Our success in creating efficient and highly active catalysts for alkyne hydration and alkene isomerization (Fig. 1), which both feature *tert*-butylated heterocycles, has spurred recent improvements from the Hintermann labs in synthesis of pyridyl halides and phosphines with *tert*-alkyl or 2,6-disubstituted aryl groups next to nitrogen [39–41]. In summary, the ability to vary catalyst structure, particularly the steric environment around the basic or coordinating nitrogen, allows one to fine-tune reactivity in many ways.

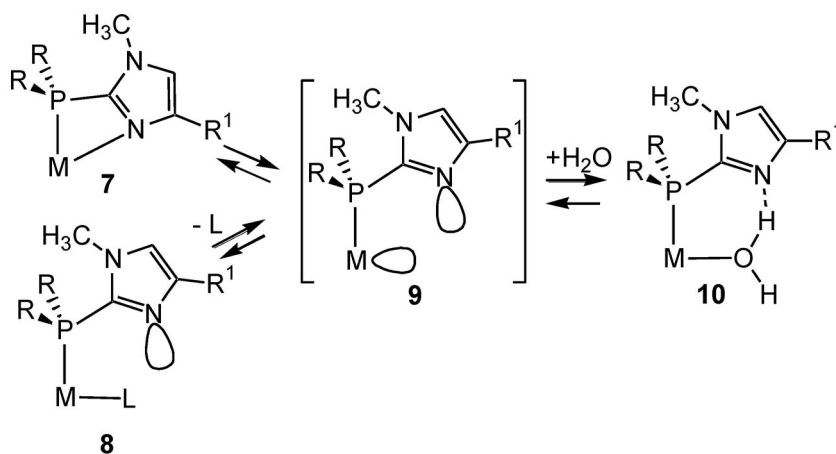


Fig. 2 Access to reactive intermediates.

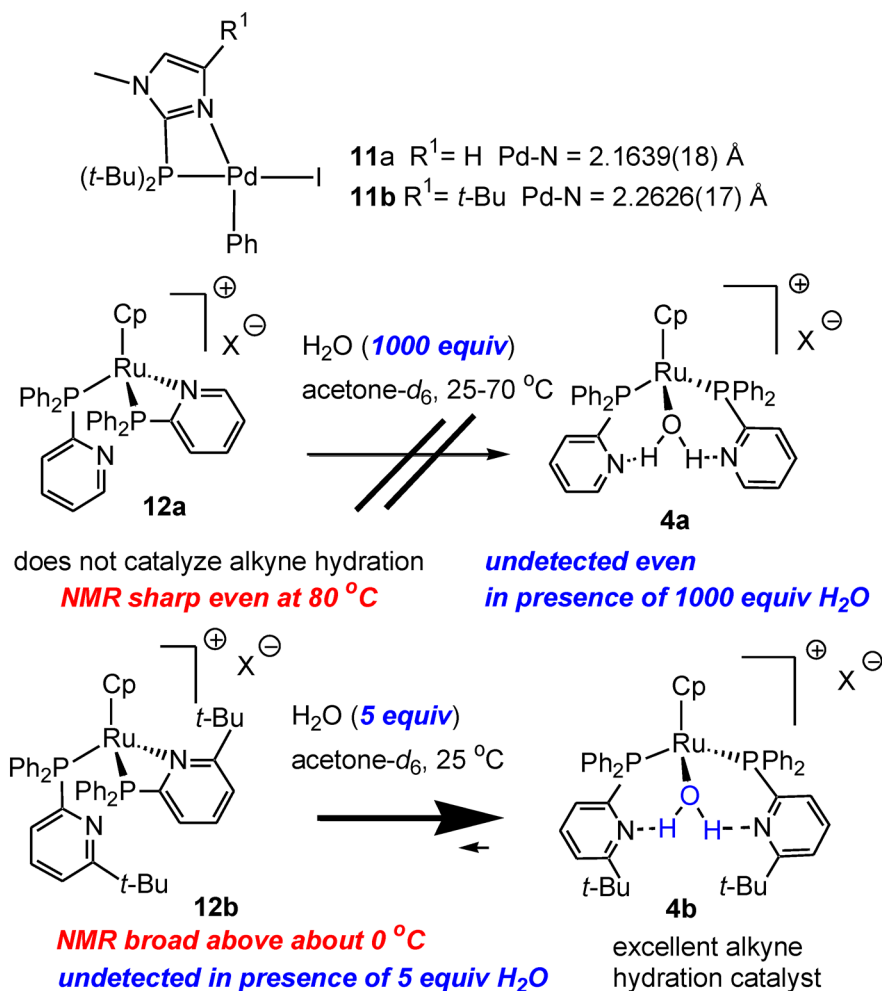


Fig. 3 Effects of steric hindrance near basic or coordinating heterocyclic nitrogen.

Anti-Markovnikov alkyne hydration

The *anti*-Markovnikov hydration of alkynes is clearly a multi-step process, whether performed by traditional [42] or bifunctional catalysts.

Because nitrile dissociation on the CpRu⁺ fragment is dissociative [43], loss of nitrile from **3** or of water from **2** or **4b** followed by alkyne coordination is the likely start of alkyne hydration. We performed a series of experiments to check effects of bifunctional ligands on both the alkyne complex structure (**13**, Fig. 4) and also subsequent isomerization [44] to vinylidene complexes (**14**). The first part of this work [30] was done using -PMe₂ ligands and acetylene, because literature reports [45] indicated that our best chance of isolating or detecting an alkyne π -complex before it isomerized to a vinylidene would occur with the smallest possible phosphine and alkyne. Moreover, we worked under dry conditions to minimize the interference from water on the process. Thus, chelate complex **12c** cooled below -40 °C in CD₂Cl₂ does not react at an appreciable rate with acetylene, but near -40 °C is converted to symmetrical π -complex **13c**, which isomerizes in high yield to vinylidene **14c** at higher temperatures (0 °C, 3 h). In contrast, control complex **13d** made and handled at room temperature isomerized to

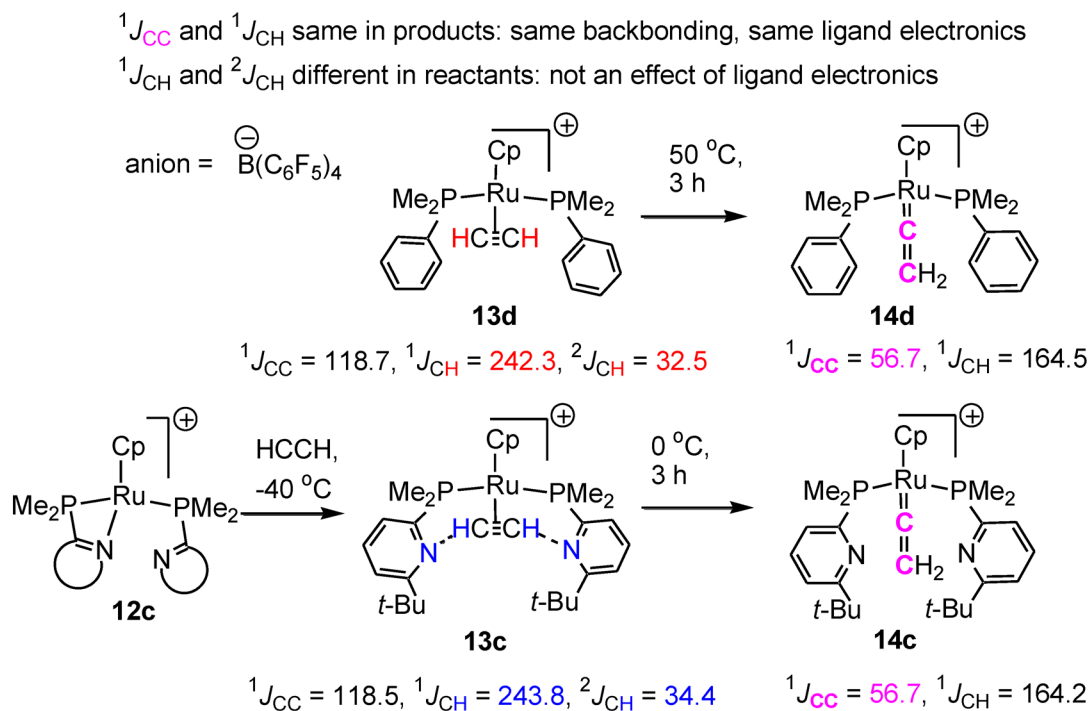


Fig. 4 Evidence for hydrogen bonding in alkyne complex **13c**.

vinylidene **14d** after 3 h of heating at 50 °C, a reaction temperature about 50 °C higher than for the bi-functional analog.

Using doubly labeled alkyne $H^{13}C^{13}CH$ allowed us to measure all possible C–H couplings in both the alkyne and vinylidene complexes. Previous work from our labs [27,31] showed that $^1J_{CC}$ could be used much as CO infrared stretching frequencies are used to discern metal–ligand backbonding and ligand electronic effects. In the vinylidene products, within experimental uncertainty $^1J_{CC}$ and $^1J_{CH}$ are the same, from which we can conclude that the ligand electronics are the same.

In distinct contrast, whereas the alkyne complex $^1J_{CC}$ values are identical within experimental uncertainty, the couplings involving alkyne hydrogens ($^1J_{CH}$ and $^2J_{CH}$) are not. Because ligand electronics is not a factor, we are left to conclude that hydrogen bonding in the pyridyl case must be responsible for the differences. Our experimental data appear to be the first for the effects of hydrogen bonding on alkyne NMR coupling constants. Searching for guidance from theory, we could find only a single paper, on $HCCH\cdots OH_2$ [46]. Reassuringly, in the complexes, comparing alkyne (**13d**) and hydrogen-bonded alkyne (**13c**), the increases in $^1J_{CH}$ and $^2J_{CH}$ seen by us experimentally (+1.5 and +1.9 Hz) resemble those predicted by comparing alkyne $HCCH$ and hydrogen-bonded alkyne in $HCCH\cdots OH_2$ (+2.55 and +1.65 Hz).

Additional evidence for hydrogen bonding in structure **13c** comes from experiments on its ^{15}N -labeled analog. Scalar couplings across hydrogen bonds are now known through a great deal of experimental and theoretical work on interactions in proteins, DNA, and supramolecular systems [47], but until our experiments there appeared to have been no use in coordination or organometallic chemistry. The $^{13}C\{^1H, ^{31}P\}$ NMR spectrum of **13c**-(^{15}N)₂, acquired at –50 °C shows a broadened doublet ($^2J_{CN} = 3 \pm 0.5$ Hz) as expected for coupling of one natural abundance acetylene ^{13}C to the nearest ^{15}N label. In none of these experiments is splitting due to $^1J_{HN}$ observed, but this value would be expected to be even smaller, less than 1 Hz.

Density functional theory (DFT) calculations on **13c** predict a slightly unsymmetrical structure with two different C–H···N angles (124.5, 135.7°) and different couplings ${}^{2h}J_{\text{CN}} = -3.4$ and -6.7 Hz, averaging to -5 Hz. The other experimentally determined NMR coupling constants for **13c** are consistently about 20 % lower than the calculated values, so -5 Hz could be multiplied by 80 % to give -4 Hz, close to the observed value. The closest literature comparison we could find came from previous theoretical work by Del Bene et al. on a simple system (NCH···NCLi) [48], but our data for **13c** appear to be the first determination for an alkyne.

The strength of the hydrogen bonds in **13c** can be gauged by calculations on conversion of **13d** to **14d** ($\Delta G = -17.9$ kcal mol $^{-1}$) and for similar conversion of **13c** to **14c** ($\Delta G = -12.7$ kcal mol $^{-1}$). Because all experimental evidence suggests no electronic difference between the phenyl and pyridyl ligands, the altered ΔG value may be attributed to thermodynamic stabilization of **13c** by two hydrogen bonds, each contributing 2.6 kcal mol $^{-1}$.

Having identified intermediate **13c** and its hydrogen bonding, we turned our attention to subsequent steps in the catalytic cycle. Although several mechanisms for alkyne to vinylidene tautomerization have been proposed [44,49], in the case of CpRu chemistry it was thought that the first step is movement of the terminal alkyne hydrogen from C1 to C2 [50–54]. However, in 2001 Tokunaga and Wakatsuki [42] showed that deuterium label at C1 was completely retained in the ultimate aldehyde product, inconsistent with simple movement of H1 to C2. To explain this unexpected result, the authors proposed initial alkyne protonation, which in the case of our phosphines could involve the heterocycle. Our bifunctional ligands clearly facilitate alkyne-to-vinylidene transformation, since the temperatures needed for this reaction are 50–90 °C lower when heterocyclic ligands are used. Preliminary calculations (Fig. 5) show possible roles for those ligands in conversion of **15** to **17**. In transition state **16**, the migrating hydrogen is within bonding distance not only of the pyridine nitrogen from which it came and of the alkyne carbon to which it is going, but also to the metal. Further work is in progress to define the roles of the heterocycle in lowering activation energies of various steps.

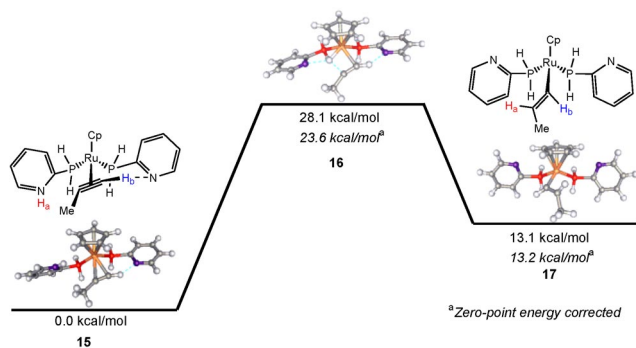


Fig. 5 Calculated structures in the reaction of propyne on a model CpRu center.

Not only does it appear that heterocyclic substituent can facilitate vinylidene formation, but also its subsequent conversion to aldehyde. Figure 6 shows the dramatic effects of heterocyclic phosphines on vinylidene reactivity. Species **18** was prepared from 1-nonyne, $\text{KB}(\text{C}_6\text{F}_5)_4$ and the same catalyst (**1**) reported as optimal by Tokunaga and Wakatsuki [21]. Bifunctional species **19** was made using **12b** and 1-nonyne. When **18** and **19** are exposed to 10 equiv of water under identical conditions, pyridylphosphine species **19** smoothly converts to nonanal and **4b** within hours, whereas **18** gives no aldehyde even after two weeks; this corresponds to an acceleration of 20000 or more. This result highlights the exceptional reactivity of vinylidene intermediate with pyridylphosphines but further experiments are needed to shed light on the mechanism.

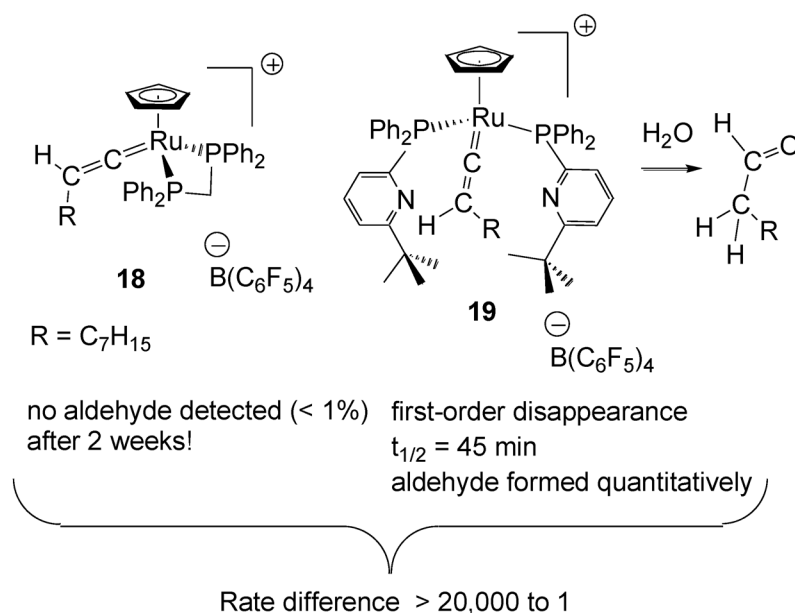


Fig. 6 Enhancement of ligand hydration by bifunctional phosphines.

Careful observation of alkyne hydration mixtures by NMR spectroscopy using either **3** or **4b** allowed us to detect catalyst **3** (when starting from **3**), **4b**, vinylidene complexes like **19**, and a fourth, unidentified species in varying amounts depending on how much alkyne had already been consumed. Eventually, after some experimentation, we were able to find conditions to maximize the amount of the fourth species. Exposure of **4b** to $\text{H}^{13}\text{C}^{13}\text{CH}$ and a limited amount of water at 0°C for several hours leads to formation of the fourth species in yields up to 91%. When allowed to react at room temperature or above, the fourth species is consumed and labeled acetaldehyde and **4b** is formed. A series of experiments including ones with ^{15}N -labeled ligands allows us to conclude that this intermediate is **23** (Fig. 7), rather than its tautomer **24**. The difference between **23** and **24** is subtle but significant: **24** bears a hydroxycarbene ligand donating a hydrogen bond to one pyridyl substituent, whereas **23** features a pyridinium moiety donating a hydrogen bond to an acyl ligand. Significant data include a very downfield ^1H resonance near 19 ppm, and for the ligand derived from $\text{H}^{13}\text{C}^{13}\text{CH}$, a downfield carbon resonance near 295 ppm and an upfield doublet at 51.4 ppm, with small C–C coupling (22.3 Hz) indicative of a single bond between the carbons. These data do not allow us to distinguish between **23** and **24**, but ^{15}N NMR data [55] (Fig. 7) do so.

Figure 7 shows that the ^{15}N shift is almost insensitive to coordination at P (**20** to **21**), or ionization of a chloride ligand or presence of a π -acidic ligand, as seen by the chemical shift for the nonchelating ligands in **12b** and **22**. On the other hand, coordination to a metal (chelating ligand in **12b**) or N-protonation (model salt **25**) lead to dramatic upfield shifts, as seen by other researchers for other metal-pyridine or pyridinium species (for examples, see [56–59]). With these background data in hand, the power of using ^{15}N NMR data to study hydrogen bonding or proton transfer is shown by considering species **4b** and **23**. In the case of **4b**, the ^{15}N chemical shift is 21.6 ppm upfield that in species **21**, showing the effects of hydrogen bonding in **4b**. Even more useful information comes from observing **23**-(^{15}N)₂ at -100°C : one ^{15}N resonance at -63.6 ppm indicates a normal pyridylphosphine with no hydrogen bonding or other interaction at the nitrogen, whereas a second resonance centered at -146.7 ppm is consistent with N-protonation (**23**) rather than a nitrogen-accepting hydrogen bond (**24**). The fact that the N-protonated nitrogen of **23** resonates near -146.7 ppm rather than near -188.5 ppm as in model pyridinium salt **25** suggests perturbation by hydrogen bonding. Additional evidence for hydrogen bond-

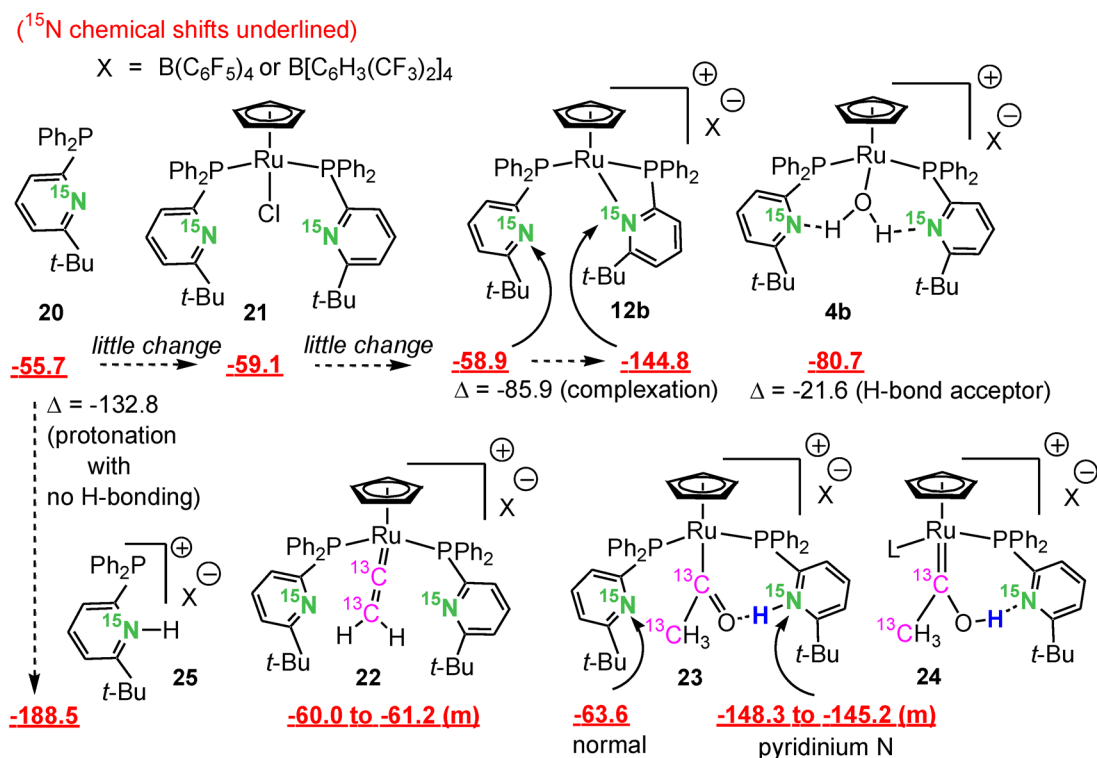


Fig. 7 ¹⁵N chemical shift data reveal protonation and hydrogen bonding in **4b** and **23**.

ing is the fact that the observed ¹⁵N–H coupling constant ¹J_{NH} for **23** (56.8 Hz) is only 62 % of that seen for **25** in CD₂Cl₂, where no hydrogen bonding occurs.

These experiments conclusively identify the protonation state of **23** and the effects of hydrogen bonding on the H–N portion of the proposed O··H–N hydrogen-bonding network, but one more piece of data is needed to unambiguously show the presence of an interaction between acyl O and pyridinium NH. Addition of D₂O to **23** (Fig. 8) in varying amounts produced mixtures of **23** and its deuterated isotopomer, where the two species exhibit dramatically different ¹³C NMR chemical shifts for the acyl carbon, which is unambiguous evidence for interaction of the acyl O with the NH/ND moiety.

We have thus identified all of the spectroscopically detectable species in the catalytic mixtures. Our ongoing work seeks to define the transition states between the observed species, as elucidated by kinetics and theoretical calculations. Modeling of the addition of water to a vinylidene ligand leading to observed acyl **23** has already revealed several distinct reaction steps, each involving proton transfer [60]; moreover, subsequent release of the aldehyde product may also involve proton transfer. Our lab is engaged in elucidating the roles of the bifunctional ligands in the remainder of the catalytic cycle.

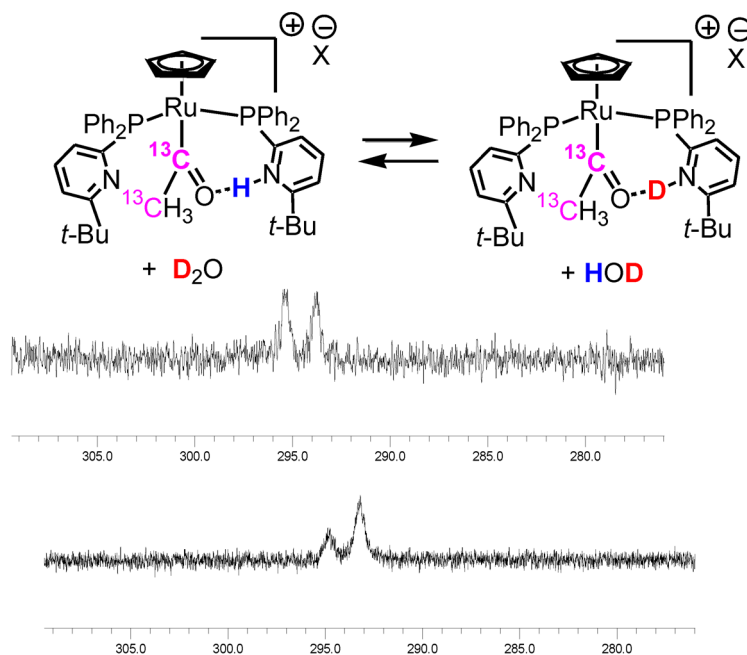


Fig. 8 Strong perturbation of ^{13}C chemical shift indicative of $\text{O}\cdots\text{H}(\text{D})\text{N}$ hydrogen bonding. The lower spectrum was acquired after additional D_2O had been added, showing $\Delta\delta_{\text{C}1} = -1.6$ ppm.

Alkene isomerization and deuteration at allylic positions

As the importance of proton transfer in alkyne hydration became apparent, we began investigating alkene isomerization facilitated by a pendant heterocycle. After screening a number of phosphines coordinated to CpRu^+ fragment, complex **6** emerged as a superior catalyst for alkene isomerization [61,62]. Notable features of **6** include its ability to move an alkene over 30 positions on an unhindered carbon chain, and its selectivity for forming and acting on (*E*)-substituted alkenes. Our mechanistic hypothesis (Fig. 9) is based on several observations, starting with the fact that addition of ethylene to **6** surprisingly leaves the chelate intact, instead resulting in one mole of free CH_3CN and a labile ethylene complex like **26**. Larger nonpolar alkenes such as those subjected to isomerization do not give detectable amounts of intermediates, but we assume that nitrile loss and alkene coordination begin the catalytic cycle. Internal deprotonation at either of the two diastereotopic allylic positions of **26** could give either **27-** or **27Z**. The high (*E*) selectivity can be explained by higher energy of diastereomer **27-Z** (with an *endo*-oriented alkyl substituent) or more likely a higher-energy transition state leading from **26-** to **27-Z**. Subsequent protonation by the imidazolium moiety at other end of the allyl intermediate would generate an isomerized alkene ligand, which could dissociate. Calculations are underway to investigate this proposed process.

Figure 9 would predict that if D_2O were present, at the stage of **27** we could expect H/D exchange and incorporation of deuterium in an alkene isomerization/deuteration process. Of the many catalysts for H/D exchange, most are effective on arene and alkane C–H bonds [63,64]. Those which perform H/D exchange at alkene C–H bonds usually do so with competing and poorly controlled alkene isomerization [65–71]. A recent exception is an iridium catalyst which does not isomerize alkenes [71]. None of these catalysts appear to act selectively at allylic positions as would be predicted by Fig. 9. Gratifyingly [32], exposure of a variety of alkenes to sufficient D_2O to give 95 % deuteration leads to nearly theoretical levels of deuteration at accessible allylic positions (Fig. 10). Propene is deuterated only at positions 1 and 3, in complete accord with Fig. 9. Longer alkenes such as 1-butene and 1-pen-

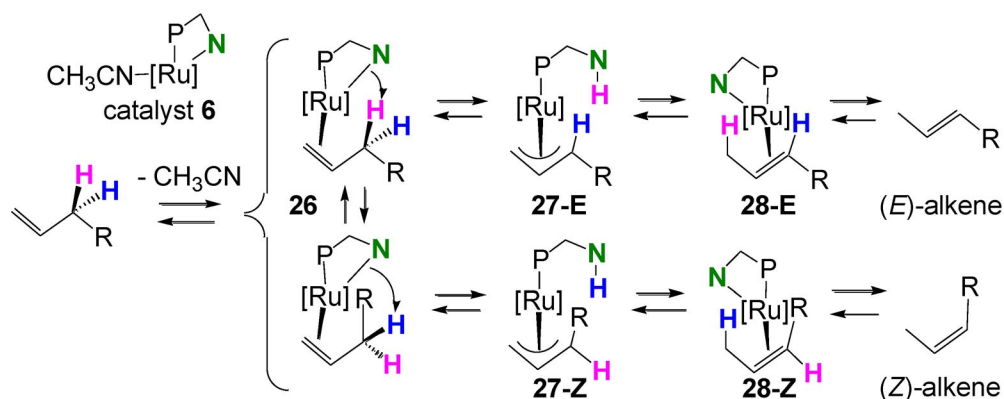


Fig. 9 Proposed mechanism of alkene isomerization by bifunctional catalyst.

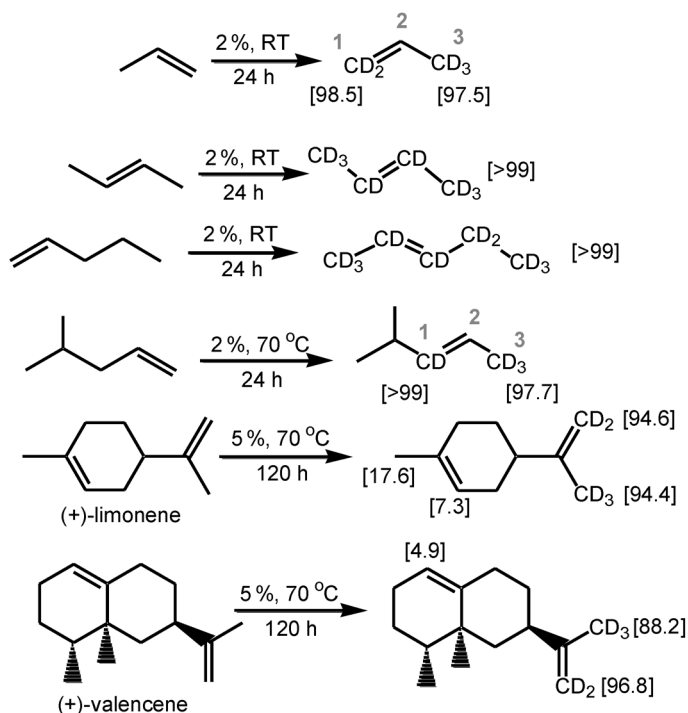


Fig. 10 Examples of selective and extensive alkene deuteration. Reactions were carried out in acetone- d_6 with enough D_2O so as to provide 20 D per exchangeable H present. The number in brackets indicates the percentage of the theoretical amount (95 %) of deuterium.

tene, however, are completely deuterated, because in these cases the catalyst can move the double bond up and down the hydrocarbon chain and make every position allylic and exchangeable. Branching impedes isomerization and hence also deuteration, in useful ways: a common alkene moiety in natural products is an exocyclic iso-propenyl group. The terpenes (+)-limonene and (+)-valencene both feature two double bonds, one within a ring and the other in an iso-propenyl substituent, and our results [32] show that the latter can be fully pentadeuterated with little deuteration elsewhere.

CONCLUSIONS

In addition to the work described above, since 2005, several notable reports of pyridylphosphine-enhanced catalysis from other labs have appeared, including in situ alkyne hydration catalysts [41], applications of *anti*-Markovnikov alkyne hydration to selective organic synthesis [72–74], and enhanced nitrile hydration [75]. Ongoing studies in the author's lab include additional applications of alkyne hydration and alkene isomerization, development of polymer-supported versions of the catalysts, and extensions of proton transfer capability to other ligand and reaction types. From all of this work, it is clear that there is much to be done and learned in the area of bifunctional catalysis involving proton transfer or hydrogen bonding.

ACKNOWLEDGMENTS

The author would like to thank all of the dedicated co-workers who are co-authors on papers cited; SDSU colleague Prof. Andrew Cooksy has been essential to advancing the computational and kinetics portions of this work; Dr. LeRoy Lafferty has assisted the author and his students with NMR experiments; Prof. Arnold Rheingold and his group have been invaluable for their X-ray diffraction expertise; and the National Science Foundation has supported not only the work described here (CHE-0415783 and -0719575), but also upgrading the SDSU departmental NMR facility (MRI CHE-0521698).

REFERENCES AND NOTES

1. C. Adams. *Chem. Ind. (London)* 740 (1999).
2. The Chemical Industry Vision2020 Technology Partnership (1996).
3. N. S. Lewis, D. G. Nocera. *Proc. Nat. Acad. Sci. USA* **103**, 15729 (2006).
4. D. B. Grotjahn, D. Combs, S. Van, G. Aguirre, F. Ortega. *Inorg. Chem.* **39**, 2080 (2000).
5. D. B. Grotjahn, C. D. Incarvito, A. L. Rheingold. *Angew. Chem., Int. Ed. Engl.* **40**, 3884 (2001).
6. For reviews of bifunctional catalysts, see (a) G. Helmchen, H. Steinhagen. *Angew. Chem., Int. Ed.* **35**, 2339 (1996); (b) E. K. van den Beuken, B. L. Feringa. *Tetrahedron* **54**, 12985 (1998); (c) G. J. Rowlands. *Tetrahedron* **57**, 1865 (2001); (d) S. E. Clapham, A. Hadzovic, R. H. Morris. *Coord. Chem. Rev.* **248**, 2201 (2004); (e) D. B. Grotjahn. *Chem.—Eur. J.* **11**, 7146 (2005); (f) T. Ikariya, K. Murata, R. Noyori. *Org. Biomol. Chem.* **4**, 393 (2006); (g) S. Das, G. W. Brudvig, R. H. Crabtree. *Chem. Commun. (Cambridge)* 413 (2008); (h) D. Natale, J. C. Mareque-Rivas. *Chem. Commun. (Cambridge)* 425 (2008); (i) D. H. Paull, C. J. Abraham, M. T. Scerba, E. Alden-Danforth, T. Lectka. *Acc. Chem. Res.* **41**, 655 (2008).
7. E. Drent, P. Arnoldy, P. H. M. Budzelaar. *J. Organomet. Chem.* **455**, 247 (1993).
8. E. Drent, P. Arnoldy, P. H. M. Budzelaar. *J. Organometal. Chem.* **475**, 57 (1994).
9. A. Scrivanti, V. Beghetto, E. Campagna, M. Zanato, U. Matteoli. *Organometallics* **17**, 630 (1998).
10. A. Dervisi, P. G. Edwards, P. D. Newman, R. P. Tooze, S. J. Colesa, M. B. Hursthouse. *J. Chem. Soc., Dalton Trans.* 1113 (1999).
11. G. R. Newkome. *Chem. Rev.* **93**, 2067 (1993).
12. Z.-Z. Zhang, H. Cheng. *Coord. Chem. Rev.* **147**, 1 (1996).
13. H. Slebocka-Tilk, J. L. Cocho, Z. Frackman, R. S. Brown. *J. Am. Chem. Soc.* **106**, 2421 (1984).
14. F.-J. Wu, D. M. Kurtz Jr., K. S. Hagen, P. D. Nyman, P. G. Debrunner, V. A. Vankai. *Inorg. Chem.* **29**, 5174 (1990).
15. C. Kimblin, W. Allen, G. Parkin. *J. Chem. Soc., Chem. Commun.* 1813 (1995).
16. T. N. Sorrell, W. E. Allen, P. S. White. *Inorg. Chem.* **34**, 952 (1995).
17. M. A. Jalil, S. Fujinami, H. Senda, H. Nishikawa. *J. Chem. Soc., Dalton Trans.* 1655 (1999).
18. F. Bachechi, A. Burini, R. Galassi, A. Macchioni, B. R. Pietroni, F. Ziarelli, C. Zuccaccia. *J. Organomet. Chem.* **593–594**, 392 (2000).

19. C. Tejel, R. Bravi, M. A. Ciriano, L. A. Oro, M. Bordonaba, C. Graiff, A. Tiripicchio, A. Burini. *Organometallics* **19**, 3115 (2000).
20. C. Tejel, M. A. Ciriano, R. Bravi, L. A. Oro, C. Graiff, R. Galassi, A. Burini. *Inorg. Chim. Acta* **347**, 129 (2003).
21. T. Suzuki, M. Tokunaga, Y. Wakatsuki. *Org. Lett.* **3**, 735 (2001).
22. D. B. Grotjahn, D. A. Lev. *J. Am. Chem. Soc.* **126**, 12232 (2004).
23. D. B. Grotjahn. *Chem.—Eur. J.* **11**, 7146 (2005).
24. D. B. Grotjahn, Y. Gong, A. G. DiPasquale, L. N. Zakharov, A. L. Rheingold. *Organometallics* **25**, 5693 (2006).
25. D. B. Grotjahn, Y. Gong, L. N. Zakharov, J. A. Golen, A. L. Rheingold. *J. Am. Chem. Soc.* **128**, 438 (2006).
26. D. B. Grotjahn, X. Zeng, A. L. Cooksy. *J. Am. Chem. Soc.* **128**, 2798 (2006).
27. D. B. Grotjahn, X. Zeng, A. L. Cooksy, W. S. Kassel, A. G. DiPasquale, L. N. Zakharov, A. L. Rheingold. *Organometallics* **26**, 3385 (2007).
28. D. B. Grotjahn. *Dalton Trans.* 6497 (2008).
29. D. B. Grotjahn, E. J. Kragulj, C. D. Zeinalipour-Yazdi, V. Miranda-Soto, D. A. Lev, A. L. Cooksy. *J. Am. Chem. Soc.* **130**, 10860 (2008).
30. D. B. Grotjahn, V. Miranda-Soto, E. J. Kragulj, D. A. Lev, G. Erdogan, X. Zeng, A. L. Cooksy. *J. Am. Chem. Soc.* **130**, 20 (2008).
31. D. B. Grotjahn, X. Zeng, A. L. Cooksy, W. S. Kassel, A. G. DiPasquale, L. N. Zakharov, A. L. Rheingold. *Organometallics* **27**, 3626 (2008).
32. G. Erdogan, D. B. Grotjahn. *J. Am. Chem. Soc.* **131**, 10354 (2009).
33. D. B. Grotjahn, D. A. Lev. *Catal. Org. React.* **104**, 227 (2005).
34. D. B. Grotjahn, J. E. Kraus, H. Amouri, M.-N. Rager, S. A. Cortes-Llamas, A. A. Mallari, A. G. DiPasquale, L. M. Liable-Sands, J. A. Golen, L. N. Zakharov, C. Moore, A. L. Rheingold. *J. Am. Chem. Soc.* (2010). Under revision.
35. M. E. Jung, G. Piizzi. *Chem. Rev.* **105**, 1735 (2005).
36. K. L. Arthur, Q. L. Wang, D. M. Bregel, N. A. Smythe, B. A. O'Neill, K. I. Goldberg, K. G. Moloy. *Organometallics* **24**, 4624 (2005).
37. V. Gallo, P. Mastrorilli, C. F. Nobile, P. Braunstein, U. Englert. *Dalton Trans.* 2342 (2006).
38. S. M. Bachrach. *J. Org. Chem.* **73**, 2466 (2008).
39. L. Hintermann, T. T. Dang, A. Labonne, T. Kribber, L. Xiao, P. Naumov. *Chem.—Eur. J.* **15**, 7167 (2009).
40. L. Hintermann, L. Xiao, A. Labonne. *Angew. Chem., Int. Ed.* **47**, 8246 (2008).
41. A. Labonne, T. Kribber, L. Hintermann. *Org. Lett.* **8**, 5853 (2006).
42. M. Tokunaga, T. Suzuki, N. Koga, T. Fukushima, A. Horiuchi, Y. Wakatsuki. *J. Am. Chem. Soc.* **123**, 11917 (2001).
43. W. Luginbühl, P. Zbinden, P. A. Pittet, T. Armbruster, H. B. Bürgi, A. E. Merbach, A. Ludi. *Inorg. Chem.* **30**, 2350 (1991).
44. Y. Wakatsuki. *J. Organomet. Chem.* **689**, 4092 (2004).
45. J. R. Lompfrey, J. P. Selegue. *J. Am. Chem. Soc.* **114**, 5518 (1992).
46. M. Pecul, J. Leszczynski, J. Sadlej. *J. Chem. Phys.* **112**, 7930 (2000).
47. S. Grzesiek, F. Cordier, V. Jaravine, M. Barfield. *Prog. Nucl. Magn. Res. Spect.* **45**, 275 (2004).
48. J. E. Del Bene, S. A. Perera, R. J. Bartlett, M. Yanez, O. Mo, J. Elguero, I. Alkorta. *J. Phys. Chem. A* **107**, 3222 (2003).
49. J. Zhu, Z. Lin. In *Metal Vinylidenes and Allenylidenes in Catalysis*, C. Bruneau, P. H. Dixneuf (Eds.), Wiley-VCH, Weinheim, Germany (2008).
50. V. Cadierno, M. P. Gamasa, J. Gimeno, C. Gonzalez-Bernardo, E. Perez-Carreno, S. Garcia-Granda. *Organometallics* **20**, 5177 (2001).
51. M. Bassetti, P. Alvarez, J. Gimeno, E. Lastra. *Organometallics* **23**, 5127 (2004).

52. M. Bassetti, V. Cadierno, J. Gimeno, C. Pasquini. *Organometallics* **27**, 5009 (2008).
53. F. De Angelis, A. Sgamellotti, N. Re. *Dalton Trans.* 3225 (2004).
54. F. De Angelis, A. Sgamellotti, N. Re. *Organometallics* **21**, 5944 (2002).
55. A footnote in Table 2 of a recent article by the author [28] gives the mistaken impression that the chemical shifts given are relative to formamide $\delta_{\text{N}} = 0$ ppm when in fact they are relative to formamide $\delta_{\text{N}} = -267.8$ ppm. It should be emphasized that for ^{15}N NMR spectroscopy there is a wide variety of reference standards and even different assignment of positive and negative signs for chemical shift changes. Neat external CH_3NO_2 has been advocated as the most reliable standard [55]; our data were acquired using a standard supplied by Varian (90 % formamide in $\text{DMSO-}d_6$) and setting its observed chemical shift as -267.8 ppm, under which conditions the ^{15}N chemical shift of CH_3NO_2 would equal 0 ppm [34,56]. J. Mason, L. F. Larkworthy, E. A. Moore. *Chem. Rev.* **102**, 913 (2002).
56. L. Pazderski, E. Szlyk, J. Sitkowski, B. Kamienski, L. Kozerski, J. Tousek, R. Marek. *Magn. Res. Chem.* **44**, 163 (2006).
57. R. Marek, A. Lycka, E. Kolehmainen, E. Sievanen, J. Tousek. *Curr. Org. Chem.* **11**, 1154 (2007).
58. R. Marek, A. Lycka. *Curr. Org. Chem.* **6**, 35 (2002).
59. D. V. Andreeva, B. Ip, A. A. Gurinov, P. M. Tolstoy, G. S. Denisov, I. G. Shenderovich, H.-H. Limbach. *J. Phys. Chem. A* **110**, 10872 (2006).
60. A. L. Cooksy. Unpublished results.
61. D. B. Grotjahn, C. R. Larsen, J. L. Gustafson, R. Nair, A. Sharma. *J. Am. Chem. Soc.* **129**, 9592 (2007).
62. D. B. Grotjahn, C. Larsen, G. Erdogan, J. Gustafson, A. Sharma, R. Nair. *Catal. Org. React.* **123**, 379 (2009).
63. T. Junk, W. J. Catallo. *Chem. Soc. Rev.* **26**, 401 (1997).
64. J. Atzrodt, V. Derdau, T. Fey, J. Zimmermann. *Angew. Chem., Int. Ed.* **46**, 7744 (2007).
65. M. H. G. Precht, M. Hoelscher, Y. Ben-David, N. Theyssen, R. Loschen, D. Milstein, W. Leitner. *Angew. Chem., Int. Ed.* **46**, 2269 (2007).
66. J. W. Faller, H. Felkin. *Organometallics* **4**, 1488 (1985).
67. J. W. Faller, C. J. Smart. *Organometallics* **8**, 602 (1989).
68. B. Rybtchinski, R. Cohen, Y. Ben-David, J. M. L. Martin, D. Milstein. *J. Am. Chem. Soc.* **125**, 11041 (2003).
69. C. M. Yung, M. B. Skaddan, R. G. Bergman. *J. Am. Chem. Soc.* **126**, 13033 (2004).
70. G. Kohl, R. Rudolph, H. Pritzkow, M. Enders. *Organometallics* **24**, 4774 (2005).
71. J. Zhou, J. F. Hartwig. *Angew. Chem., Int. Ed.* **47**, 5783 (2008).
72. T. Kribber, A. Labonne, L. Hintermann. *Synthesis* 2809 (2007).
73. A. Labonne, L. Zani, L. Hintermann, C. Bolm. *J. Org. Chem.* **72**, 5704 (2007).
74. L. Hintermann, T. Kribber, A. Labonne, E. Paciok. *Synlett* 2412 (2009).
75. T. Oshiki, H. Yamashita, K. Sawada, M. Utsunomiya, K. Takahashi, K. Takai. *Organometallics* **24**, 6287 (2005).